

Article

Comprehensive Profiling of Mutations to Influenza Virus PB2 That Confer Resistance to the Cap-Binding Inhibitor Pimodivir

Y. Q. Shirleen Soh ^{1,2}, Keara D. Malone ¹, Rachel T. Eguia ¹ and Jesse D. Bloom ^{1,2,3,*} 

¹ Fred Hutchinson Cancer Research Center, Basic Sciences Division, Seattle, WA 98109, USA; yqsoh@fredhutch.org (Y.Q.S.S.); kmalone2@fredhutch.org (K.D.M.); reguia@fredhutch.org (R.T.E.)

² Fred Hutchinson Cancer Research Center, Computational Biology Program, Seattle, WA 98109, USA

³ Howard Hughes Medical Institute, Seattle, WA 98109, USA

* Correspondence: j bloom@fredhutch.org

Abstract: Antivirals are used not only in the current treatment of influenza but are also stockpiled as a first line of defense against novel influenza strains for which vaccines have yet to be developed. Identifying drug resistance mutations can guide the clinical deployment of the antiviral and can additionally define the mechanisms of drug action and drug resistance. Pimodivir is a first-in-class inhibitor of the polymerase basic protein 2 (PB2) subunit of the influenza A virus polymerase complex. A number of resistance mutations have previously been identified in treated patients or cell culture. Here, we generate a complete map of the effect of all single-amino-acid mutations to an avian PB2 on resistance to pimodivir. We identified both known and novel resistance mutations not only in the previously implicated cap-binding and mid-link domains, but also in the N-terminal domain. Our complete map of pimodivir resistance thus enables the evaluation of whether new viral strains contain mutations that will confer pimodivir resistance.



Citation: Soh, Y.Q.S.; Malone, K.D.; Eguia, R.T.; Bloom, J.D. Comprehensive Profiling of Mutations to Influenza Virus PB2 That Confer Resistance to the Cap-Binding Inhibitor Pimodivir. *Viruses* **2021**, *13*, 1196. <https://doi.org/10.3390/v13071196>

Academic Editor: Craig McCormick

Received: 15 May 2021
Accepted: 17 June 2021
Published: 22 June 2021

Publisher's Note: MDPI stays neutral with regard to jurisdictional claims in published maps and institutional affiliations.



Copyright: © 2021 by the authors. Licensee MDPI, Basel, Switzerland. This article is an open access article distributed under the terms and conditions of the Creative Commons Attribution (CC BY) license (<https://creativecommons.org/licenses/by/4.0/>).

Keywords: influenza; drug resistance; pimodivir; PB2; polymerase; deep mutational scanning

1. Introduction

Antivirals are an important prophylactic and treatment for influenza, particularly for high-risk patients and those with severe infections [1]. They are also stockpiled as a first line of defense against pandemics caused by novel influenza strains [2], for which vaccines are unlikely to be available for many months.

The first influenza antivirals approved over two decades ago are the adamantanes, which target the matrix 2 (M2) ion channel of influenza A viruses, and neuraminidase inhibitors (NAIs), which inhibit the viral enzyme that facilitates the release of viral progeny from infected cells [3]. Their clinical use, however, has been impacted by the emergence of resistance mutations. Consequently, adamantanes are no longer recommended for clinical use due to resistance in currently circulating influenza strains [4]. NAIs remain the standard of care, though resistance has been shown to emerge in some patients [5], and went to fixation in the now extinct lineage of H1N1 influenza that circulated in humans prior to 2009 [6]. As such, there is an important need for new antivirals that not only extend the clinically beneficial window of treatment but are also effective against adamantane- and NAI-resistant strains.

In recent years, efforts have focused on a new class of antiviral drugs for influenza directed against the influenza polymerase [7,8]. The influenza polymerase is an attractive antiviral target because it plays a pivotal role in the replication and transcription of the viral genome and is highly conserved [9,10]. Baloxavir and favipiravir are the first developed antivirals in this class [11,12]. Baloxavir targets the endonuclease function of the polymerase acidic protein (PA) subunit of the influenza polymerase, thus preventing the transcription of the viral mRNA [13]. Favipiravir is a nucleoside analog that induces chain termination and lethal mutagenesis during viral genome replication [14,15].

Pimodivir (also known as VX-787) is also a member of this new class of antivirals targeting the influenza polymerase complex [16]. Specifically, pimodivir targets the PB2 subunit of the polymerase, preventing its binding to the 7-methyl GTP caps of host-capped mRNAs, thus ultimately inhibiting the first step of viral gene transcription. Importantly, pimodivir is active against a diverse panel of influenza A virus strains, including H5N1 avian influenza [17], highlighting its potential as a first-line treatment against novel pandemic strains.

Identifying resistance mutations can guide the clinical deployment of appropriate antivirals and aid in developing new antivirals that are less susceptible to resistance. Known resistance mutations to pimodivir, as with previous influenza antivirals, have typically been identified one at a time as they arose over the course of antiviral treatment either in patients or in the laboratory in cell culture [16–23]. These mutations are located primarily in the PB2 7-methyl GTP cap-binding pocket [17], as well as the mid-link domain where additional contacts with pimodivir are made [24,25]. However, these mutations likely do not represent the full range of mutations that affect pimodivir resistance.

Here, we fully map pimodivir resistance mutations in high throughput. Specifically, using deep mutational scanning, we quantified how pimodivir resistance was affected by all amino-acid mutations to an avian influenza PB2 that were compatible with viral replication in human cells.

2. Materials and Methods

2.1. PB2 Mutant Virus Libraries

We previously generated three independent mutant virus libraries containing all single amino-acid-mutations to PB2 from an avian influenza strain [26]. The PB2 mutations were made on a background of reassortant virus using polymerase and nucleoprotein genes (PB2, PB1, PA, NP) from the avian influenza strain A/Green-winged Teal/Ohio/175/1986 (S009) [27], and remaining genes (HA, NA, M, NS) from A/WSN/1933 (H1N1) [28]. These libraries were passaged in A549 cells to select for viruses that encoded all functionally tolerated mutations in PB2 for viral replication in A549 cells. The resulting functional virus was used here for resistance profiling.

2.2. Resistance Profiling

To identify resistance mutations, we passaged the mutant virus libraries in A549 cells in the absence or presence of pimodivir, and then identified the mutant viruses that were enriched upon drug selection using deep sequencing. We aimed to passage 1×10^6 TCID₅₀ of each mutant virus library in A549 cells at an MOI of 0.2 in the presence of 50 nM of pimodivir. 4 h prior to infection, we seeded 5×10^6 cells in D10 in a 15 cm dish. Just prior to the infection, we replaced D10 media with WGM with 50 nM of pimodivir. 1×10^6 TCID₅₀ of each virus library was then added to each plate. At 2 h post-infection, we replaced the inoculum with fresh WGM with 50 nM pimodivir. 44 h post-infection, we harvested the viral supernatant. As mock-selected controls, each mutant virus library was also similarly passaged in the absence of pimodivir. Selected and mock-selected viral supernatants were sequenced with a barcoded subamplicon sequencing approach as previously described [26,29].

2.3. Analysis of Deep Sequencing Data

Deep mutational scanning sequence data was analyzed using dms_tools2 (https://jbloomlab.github.io/dms_tools2, v. 2.3.0, accessed on 14 April 2021). The differential selection [30] was quantified as the logarithm of the mutation's enrichment in the pimodivir-selected mutant virus library relative to the mock-selected control library. Sequencing of wildtype DNA plasmid was used as the error control for calculating differential selection.

2.4. Data Availability and Source Code

The codes for the analyses are provided as Supplemental File S1 and at https://github.com/jbloombloom/PB2_Pimodivir_Resistance (accessed on 4 June 2021). Mean mutation and site differential selection measurements are provided as Supplemental Files S2 and S3, respectively. Sequencing reads are deposited into the NCBI SRA under BioProject ID PRJNA719471.

2.5. Polymerase Activity Assays

Minigenome assays were performed in biological triplicate (starting from independent bacterial clones of each PB2 mutant) in HEK293T cells. We seeded 2.5×10^4 HEK293T cells per well of a 96-well plate. Cells were transfected the next day with 10 ng each of HDM_S009_PB2 (for the respective mutant), HDM_S009_PB1, HDM_S009_PA, HDM_S009_NP, 30 ng of pHH-PB1-flank-eGFP reporter, and 30 ng of pcDNA-mCherry as the transfection control using BioT. At 22 h post-transfection, cells were trypsinized and analyzed by flow cytometry. We report minigenome activity as the percent of mCherry-positive cells that are GFP-positive.

2.6. Analysis of PB2 Sequence Variation

Sequences of recent influenza strains were downloaded from the Influenza Virus Resource Database in June 2021. Full coding sequences were obtained for human H3N2 seasonal influenza (sequences collected from 2015–2021), human pandemic H1N1 influenza (2015–2021), all subtypes of avian influenza (2015–2021), and human infections of H5N1 and H7N9 avian influenza strains (all sequences available). Unique sequences were aligned using phydms_prealignment (http://jbloomlab.github.io/phydms/phydms_prealignment.html, accessed on 14 April 2021). The sequences, alignments, and analysis are available at https://github.com/jbloombloom/PB2_Pimodivir_Resistance (accessed on 4 June 2021).

3. Results

In a prior study, we generated triplicate mutant virus libraries containing all single-amino-acid mutations to PB2 from an avian influenza strain, S009, with the other polymerase complex genes (PB1, PA, and NP) also derived from S009, and the remaining genes derived from the lab-adapted A/WSN/1933 (H1N1) strain [26]. We passaged each library to obtain viruses capable of replication in the A549 human lung epithelial carcinoma cell line [26]. In the present study, we passaged these mutant virus libraries once more in A549 cells in the presence or absence of 50 nM of pimodivir, a concentration chosen so that only a small fraction (1–10%) of viral titers was recovered compared to a mock selection (Figure S1A). To quantify the effect of each mutation on viral growth in the presence of pimodivir, we sequenced the passaged viruses and then calculated the enrichment of each mutation in the pimodivir-selected vs. nonselected conditions. This value, termed hereafter the “differential selection”, reflects how favorable a mutation is in the presence over the absence of pimodivir.

Selection of pimodivir resistance mutations was highly reproducible across three biological replicates (Figure S1B). In addition to previously identified resistance mutations, we identified many more mutations, both at sites at which mutations were previously found, as well as new sites (Figure 1 and Figure S2). Many of these mutations are evolutionarily accessible by single nucleotide substitutions from currently circulating PB2 sequences (Figure 1B–E). Resistance mutations occur in three regions of the PB2 protein.

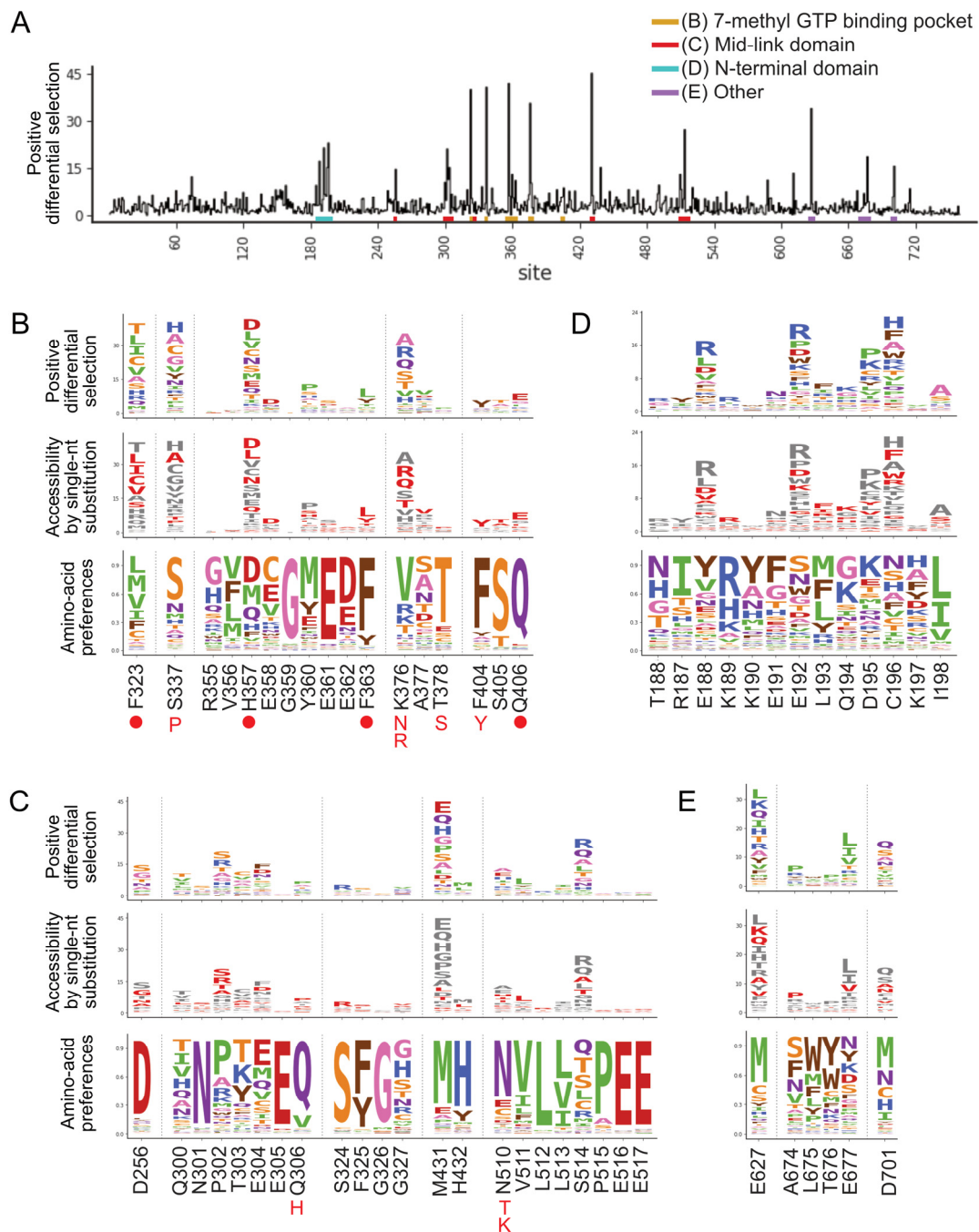


Figure 1. A complete map of pimodivir resistance. (A) Positive site differential selection across the entire PB2 protein. Regions of interest from different domains are underlined in different colors. (B–E) Mutation-level profiles for regions of interest in the (B) 7-methyl GTP binding pocket, (C) mid-link domain, (D) N-terminal domain, (E) other regions of PB2. The top plot of each panel shows the positive differential selection profile, where the height of each amino acid is proportional to its differential selection. The middle plot shows which amino acids are accessible by single-nucleotide substitution from existing avian PB2 sequences. Accessible amino acids are shown in red. The bottom plot shows the amino acid preferences at each site in human A549 cells, as previously measured in [26]. The preference for an amino acid is proportional to its enrichment during the prior functional selection of the complete PB2 mutant library in A549 cells. The height of each letter is proportional to the preference for that amino acid at that site. Sites of known resistance mutations are indicated by either a circle underneath the site or the specific resistance mutation if it is known.

The first region is the 7-methyl GTP cap-binding pocket (Figures 1B and 2A, Figure S3A). Resistance mutations in this region, in combination with structural stud-

ies, provide support for the proposed mechanism that pimodivir occupies this pocket and interacts with PB2 similarly to the m⁷GTP guanine base [17]. Resistance mutations previously identified in this region are located at sites K376, which forms hydrogen bonds to both m⁷GTP and pimodivir, H357, F404, and F323, which form aromatic side chain interactions with the azaindole and pyrimidine rings of pimodivir, Q406, which interacts with the carboxylic acid of pimodivir, as well as sites S337, F363, and T378. For each of these sites with known resistance mutations, we identify additional substitutions at each of these sites that also confer resistance, e.g., sites 337 and 376. Sites that appear more tolerant of mutations, e.g., H357, have a correspondingly larger number of resistance mutations at that site, and vice versa, e.g., F404 (Figure 1B).

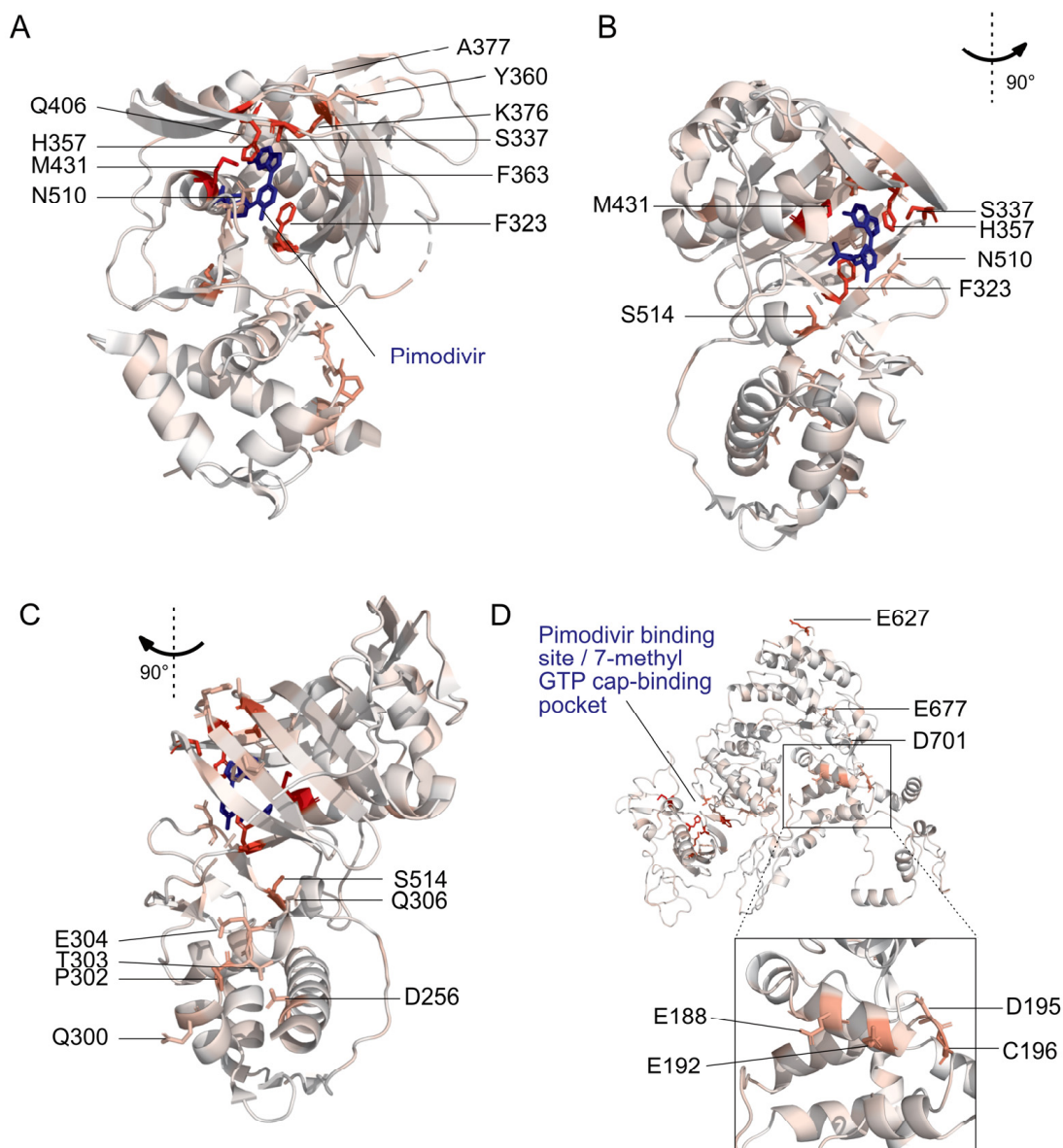


Figure 2. Locations of pimodivir resistance mutations on the PB2 protein. Amino acids are colored on a scale of white to red according to the total positive differential selection at that site, with red corresponding to a high differential selection. Sites of interest, as identified in Figure 1, are labeled. (A–C) Structural model of PB2 cap-mid-link double domain with pimodivir in the transcriptionally inactive “apo” configuration [25]. Sites with resistance mutations that are in the 7-methyl GTP binding pocket and mid-link domain are labeled here. PDB: 6EUV. (D) Structural model of full length PB2 in the apo configuration, but without pimodivir [31]. Sites of resistance mutations that are in the N-terminal domain and elsewhere are labeled here. PDB: 5D98. Supplemental Figure S3 accompanies this figure.

The second region is the mid-link domain (Figures 1C and 2B,C, Figure S3B,C). Previous studies had identified resistance mutations, such as N510T [17], that lie outside the cap-binding pocket. A more recent structural characterization of pimodivir in complex with the PB2 protein cap-binding and mid-link domain revealed that in the presence of pimodivir, the polymerase can also take up the transcriptionally inactive “apo” configuration. In this configuration, the mid-link and cap-binding domain are stabilized by interdomain interactions, as well as by contacts between pimodivir and the mid-link domain [24,25]. Pimodivir binding is thus proposed to have a second indirect mode of action that is the stabilization of this transcriptionally inactive “apo” state, thus occluding this cap-binding pocket. In support of this model, we identify numerous mutations at sites postulated to play a role in stabilizing the inhibitor bound “apo” state, such as at site N510. We also identify resistance mutations at sites such as S514, which do not appear to directly contact pimodivir but are in proximity to other segments of the mid-link domain. The substitution of serine by various bulky side-chains, such as arginine and glutamine, may destabilize the interaction between the cap-binding and mid-link domain, countering the stabilizing effect of pimodivir.

Unexpectedly, we identified resistance mutations in the PB2 N-terminal domain, such as at sites E188, E192, D195, and C196, located far away from where pimodivir binds (Figures 1D and 2D, Figure S3D). Strikingly, E188 and E195 are located side by side on an outward-facing side of an alpha-helix, and D195 and C196 are on an adjacent loop that is also on the surface of the PB2 protein. The most selected amino acids at these sites in the presence of pimodivir are basic amino acids including arginine, histidine, and lysine. Further investigation will be needed to fully understand the role of these sites in pimodivir resistance. Additionally, we also identified sites of high positive differential selection at sites known to be important in human adaptation, namely 627 and 701 (Figure 1E). Thus, it appears that in the context of an avian influenza PB2, human adaptive mutations confer an advantage for influenza replication in human cells in the presence of pimodivir.

To validate that our high-throughput approach accurately identified mutations that countered the inhibitory effects of pimodivir on polymerase activity, we quantified the effect of mutations in a minigenome assay in the presence of a range of pimodivir concentrations (Figure 3A–C). We individually validated a selection of mutations from each of the three regions described above. A few new mutations were selected from two sites at which prior resistance mutations had been identified (F323L, H357D, M431E), and the remaining mutations were in sites that had not yet been associated with pimodivir resistance. Each mutation was made on the background of PB2 from the S009 avian influenza strain that had the E627K human-adaptive mutation. All mutations selected for validation increased pimodivir resistance, raising the EC_{50} between 2 to almost 30-fold (Figure 3E). Some of the resistance mutations, particularly those in the mid-link domain, appear to be detrimental to minigenome activity (Figure 3D). Hence, there may exist a trade-off between resistance to pimodivir and baseline polymerase activity.

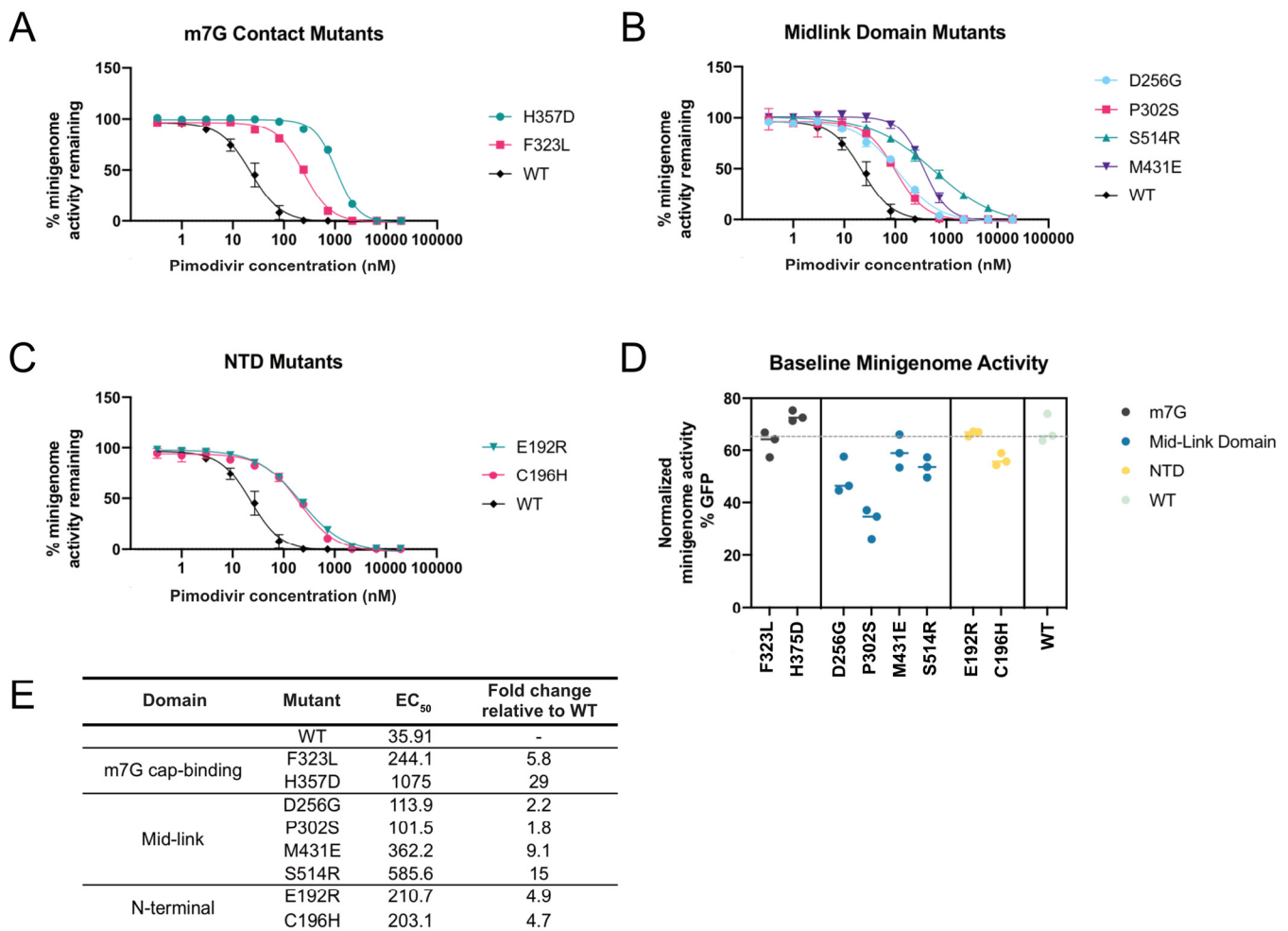


Figure 3. Validation of pimodivir resistance mutations using a minigenome assay. The indicated mutations were all made in the background of PB2-S009 with the E627K human-adaptive mutation. Hence, the “wildtype control”, “WT”, refers to PB2 that already has the E627K mutation. (A–C) Minigenome activity curves were plotted based on minigenome activity at various pimodivir concentrations, normalized to activity in the absence of pimodivir. (D) Minigenome activity was measured for polymerases containing each of the mutations, in the absence of pimodivir. (E) EC₅₀ and fold-change in EC₅₀ relative to wildtype, determined from the fit four-parameter logistic curves.

Finally, we asked whether PB2 resistance mutations, especially those new ones identified here, may already exist in circulating influenza strains. We examined PB2 sequences from all subtypes of avian influenza, human-infecting avian influenza (H5N1 and H7N9), as well as seasonal and pandemic influenza (H3N2 and H1N1), looking closely at sites associated with pimodivir resistance (Figure 4). Consistent with previous reports, we found that PB2 was very well-conserved. Pimodivir resistance mutations are not observed at significant frequencies in any of the strains analyzed. Hence, we expect pimodivir to be effective against these examined strains. We note, however, that many pimodivir resistance mutations are evolutionarily accessible by single nucleotide substitutions from currently circulating PB2 sequences. Therefore, surveillance efforts are critical for the early identification of any resistant influenza variants as they arise.



Figure 4. Natural sequence variation at sites of pimodivir resistance. Logoplots representing mutation differential selection under pimodivir selection (top row) and amino acid frequencies in various influenza strains (remaining rows). For the plot representing the mutation differential selection, the height of each amino acid is proportional to its differential selection. For the plots representing the amino acid frequency, the height of each amino acid is proportional to its frequency observed in the specified influenza strains.

4. Discussion

We have quantified how pimodivir resistance is affected by all single-amino-acid mutations to an avian influenza PB2 that are compatible with viral replication in human cells. Our comprehensive mapping identified not only many previously known resistance mutations but also new mutations at previously identified sites and new sites. The identified mutations in the cap-binding and mid-link regions of the PB2 protein lend support to current proposed mechanisms of drug action and thus resistance, namely that of the direct

inhibition of capped-RNA binding [17], as well as the indirect stabilization of the transcriptionally inactive apo configuration of the cap-binding and mid-link domains [24,25].

A third set of mutations in the PB2 N-terminal domain is unexplained by existing models of pimodivir action. Their characteristics suggest that they may interact with other domains or subunits of the polymerase or other proteins—based on existing structures, they do not contact pimodivir directly. The sites of these mutations (E188, E192, D195, C196) are in a tight cluster on the surface of the protein. Finally, basic amino acids appear to be favored across these sites.

In our current study, we have thus identified numerous novel pimodivir resistance mutations and validated several of them by a minigenome polymerase assay. Further studies, including the validation and characterization of these resistance mutations in a recombinant virus, will be required to understand how these mutations confer pimodivir resistance.

Finally, our comprehensive map of resistance mutations provides empirical data with which we can evaluate new viral strains for pimodivir resistance, including those mutations that would not have been predicted by structural analyses. This in turn will enable the rapid determination of the best antiviral approach to be clinically deployed.

We began this work while pimodivir was in active development and in the midst of Phase 3 clinical trials. Recently, in September 2020, the development of pimodivir for the treatment of influenza was halted due to interim analyses of Phase 3 data that showed that pimodivir, while effective, did not demonstrate an added benefit to the current standard of care (<https://www.janssen.com/janssen-discontinue-pimodivir-influenza-development-program>, accessed on 4 June 2021). Our pimodivir resistance map, while not immediately applicable at the moment to an approved antiviral therapy, is nevertheless useful in the case that resistance against existing antivirals leads us to revisit pimodivir as an alternate antiviral. Further, such maps of antiviral resistance may help us design the next generation of PB2 inhibitors that are less susceptible to the evolution of resistance. More generally, we demonstrate the utility of deep mutational scanning in evaluating drug resistance and thus facilitating informed clinical responses during pandemic outbreaks.

Supplementary Materials: The following are available online at <https://www.mdpi.com/article/10.3390/v13071196/s1>, Figure S1: (A) The fraction of virus that survived pimodivir selection, as calculated by TCID50 recovered relative to the mock selected condition. (B) Correlations between the positive site differential selection for biological triplicates, Figure S2: Complete mutation-level resistance profile across PB2. The height of each amino acid is proportional to its differential selection, Figure S3: Locations of pimodivir resistance mutations on the PB2 protein. Sites of high differential selection are colored red, as identified in Figure 1, and all other sites are colored white for simplicity. File S1: Code and results for computational analyses, File S2: Mean mutation differential selection measurements for pimodivir selection, File S3: Mean mutation and site differential selection measurements for pimodivir selection.

Author Contributions: Conceptualization, Y.Q.S.S. and J.D.B.; investigation, Y.Q.S.S., K.D.M. and R.T.E.; resources, writing—original draft preparation, Y.Q.S.S.; writing—review and editing, Y.Q.S.S., K.D.M., R.T.E. and J.D.B. All authors have read and agreed to the published version of the manuscript.

Funding: This research was supported by the NIAID of the NIH to J.D.B. (R01AI127893 and R01AI141707), the Damon Runyon Cancer Research Foundation to Y.Q.S.S. (DRG-2271-16), and the Mahan Postdoctoral Fellowship to Y.Q.S.S., J.D.B. is an Investigator of the Howard Hughes Medical Institute.

Institutional Review Board Statement: Not applicable.

Informed Consent Statement: Not applicable.

Data Availability Statement: Code for the analyses is provided as Supplemental File S1 and at https://github.com/jbloomlab/PB2_Pimodivir_Resistance (accessed on 4 June 2021). Mean mutation and site differential selection measurements are provided as Supplemental Files S2 and S3, respectively. Sequencing reads are deposited into the NCBI SRA under BioProject ID PRJNA719471.

Acknowledgments: We thank Jeffrey Taubenberger for providing plasmids for A/Green-winged Teal/Ohio/175/1986 (S009), and Andrew Mehle and Steven Baker for advice about growing virus containing S009 polymerase and NP genes. We thank William Fowler for help with molecular cloning.

Conflicts of Interest: J.D.B. consults for Moderna on viral evolution, Flagship Labs 77 on deep mutational scanning, and has the potential to receive a share of IP revenue as an inventor on a Fred Hutch licensed technology/patent (application WO2020006494) related to deep mutational scanning of viral proteins. The funders had no role in the design of the study; in the collection, analyses, or interpretation of data; in the writing of the manuscript, or in the decision to publish the results.

References

1. Nguyen-Van-Tam, J.S.; Bresee, J. Pandemic preparedness and response. In *Textbook of Influenza*; John Wiley & Sons, Ltd.: Oxford, UK, 2013; pp. 453–469.
2. Patel, T.S.; Cinti, S.; Sun, D.; Li, S.; Luo, R.; Wen, B.; Gallagher, B.A.; Stevenson, J.G. Oseltamivir for pandemic influenza preparation: Maximizing the use of an existing stockpile. *Am. J. Infect. Control.* **2017**, *45*, 303–305. [[CrossRef](#)]
3. Hurt, A.C.; Ho, H.-T.; Barr, I. Resistance to anti-influenza drugs: Adamantanes and neuraminidase inhibitors. *Expert Rev. Anti-infective Ther.* **2006**, *4*, 795–805. [[CrossRef](#)]
4. Bright, R.A.; Medina, M.; Xu, X.; Perez-Oronoz, G.; Wallis, T.R.; Davis, X.M.; Povinelli, L.; Cox, N.J.; Klimov, A.I. Incidence of adamantane resistance among influenza A (H3N2) viruses isolated worldwide from 1994 to 2005: A cause for concern. *Lancet* **2005**, *366*, 1175–1181. [[CrossRef](#)]
5. Lee, N.; Hurt, A.C. Neuraminidase inhibitor resistance in influenza: A clinical perspective. *Curr. Opin. Infect. Dis.* **2018**, *31*, 520–526. [[CrossRef](#)]
6. Bloom, J.; Gong, L.I.; Baltimore, D. Permissive Secondary Mutations Enable the Evolution of Influenza Oseltamivir Resistance. *Science* **2010**, *328*, 1272–1275. [[CrossRef](#)]
7. Takashita, E. Influenza Polymerase Inhibitors: Mechanisms of Action and Resistance. *Cold Spring Harb. Perspect. Med.* **2021**, *11*, a038687. [[CrossRef](#)]
8. Hayden, F.G.; Shindo, N. Influenza virus polymerase inhibitors in clinical development. *Curr. Opin. Infect. Dis.* **2019**, *32*, 176–186. [[CrossRef](#)] [[PubMed](#)]
9. Einfeld, A.J.; Neumann, G.; Kawaoka, Y. At the centre: Influenza A virus ribonucleoproteins. *Nat. Rev. Genet.* **2015**, *13*, 28–41. [[CrossRef](#)] [[PubMed](#)]
10. Te Velthuis, A.J.W.; Fodor, E. Influenza virus RNA polymerase: Insights into the mechanisms of viral RNA synthesis. *Nat. Rev. Microbiol.* **2016**, *14*, 479–493. [[CrossRef](#)] [[PubMed](#)]
11. O’Hanlon, R.; Shaw, M.L. Baloxavir marboxil: The new influenza drug on the market. *Curr. Opin. Virol.* **2019**, *35*, 14–18. [[CrossRef](#)] [[PubMed](#)]
12. Shiraki, K.; Daikoku, T. Favipiravir, an anti-influenza drug against life-threatening RNA virus infections. *Pharmacol. Ther.* **2020**, *209*, 107512. [[CrossRef](#)]
13. Hayden, F.G.; Sugaya, N.; Hirotsu, N.; Lee, N.; De Jong, M.D.; Hurt, A.C.; Ishida, T.; Sekino, H.; Yamada, K.; Portsmouth, S.; et al. Baloxavir Marboxil for Uncomplicated Influenza in Adults and Adolescents. *N. Engl. J. Med.* **2018**, *379*, 913–923. [[CrossRef](#)] [[PubMed](#)]
14. Furuta, Y.; Takahashi, K.; Fukuda, Y.; Kuno, M.; Kamiyama, T.; Kozaki, K.; Nomura, N.; Egawa, H.; Minami, S.; Watanabe, Y.; et al. In Vitro and In Vivo Activities of Anti-Influenza Virus Compound T-705. *Antimicrob. Agents Chemother.* **2002**, *46*, 977–981. [[CrossRef](#)]
15. Baranovich, T.; Wong, S.-S.; Armstrong, J.; Marjuki, H.; Webby, R.J.; Webster, R.G.; Govorkova, E.A. T-705 (Favipiravir) Induces Lethal Mutagenesis in Influenza A H1N1 Viruses In Vitro. *J. Virol.* **2013**, *87*, 3741–3751. [[CrossRef](#)] [[PubMed](#)]
16. Clark, M.P.; Ledebor, M.W.; Davies, I.; Byrn, R.A.; Jones, S.M.; Perola, E.; Tsai, A.; Jacobs, M.; Nti-Addae, K.; Bandarage, U.K.; et al. Discovery of a Novel, First-in-Class, Orally Bioavailable Azaindole Inhibitor (VX-787) of Influenza PB2. *J. Med. Chem.* **2014**, *57*, 6668–6678. [[CrossRef](#)] [[PubMed](#)]
17. Byrn, R.A.; Jones, S.M.; Bennett, H.B.; Bral, C.; Clark, M.P.; Jacobs, M.D.; Kwong, A.D.; Ledebor, M.W.; Leeman, J.R.; McNeil, C.F.; et al. Preclinical activity of VX-787, a first-in-class, orally bioavailable inhibitor of the influenza virus polymerase PB2 subunit. *Antimicrob. Agents Chemother.* **2015**, *59*, 1569–1582. [[CrossRef](#)] [[PubMed](#)]
18. Trevejo, J.M.; Asmal, M.; Vingerhoets, J.; Polo, R.; Robertson, S.; Jiang, Y.; Kieffer, T.L.; Leopold, L. Pimodivir treatment in adult volunteers experimentally inoculated with live influenza virus: A Phase IIa, randomized, double-blind, placebo-controlled study. *Antivir. Ther.* **2018**, *23*, 335–344. [[CrossRef](#)]
19. Finberg, R.W.; Lanno, R.; Anderson, D.; Fleischhackl, R.; Van Duijnhoven, W.; Kauffman, R.S.; Kosoglou, T.; Vingerhoets, J.; Leopold, L. Phase 2b Study of Pimodivir (JNJ-63623872) as Monotherapy or in Combination With Oseltamivir for Treatment of Acute Uncomplicated Seasonal Influenza A: TOPAZ Trial. *J. Infect. Dis.* **2018**, *219*, 1026–1034. [[CrossRef](#)]
20. Gregor, J.; Radilová, K.; Brynda, J.; Fanfrlík, J.; Konvalinka, J.; Kožíšek, M. Structural and Thermodynamic Analysis of the Resistance Development to Pimodivir (VX-787), the Clinical Inhibitor of Cap Binding to PB2 Subunit of Influenza A Polymerase. *Molecules* **2021**, *26*, 1007. [[CrossRef](#)]

21. Mengual-Chuliá, B.; Alonso-Cordero, A.; Cano, L.; Mosquera, M.D.M.; de Molina, P.; Vendrell, R.; Reyes-Prieto, M.; Jané, M.; Torner, N.; Martínez, A.I.; et al. Whole-Genome Analysis Surveillance of Influenza A Virus Resistance to Polymerase Complex Inhibitors in Eastern Spain from 2016 to 2019. *Antimicrob. Agents Chemother.* **2021**, *65*, e02718-20. [[CrossRef](#)]
22. Omoto, S.; Speranzini, V.; Hashimoto, T.; Noshi, T.; Yamaguchi, H.; Kawai, M.; Kawaguchi, K.; Uehara, T.; Shishido, T.; Naito, A.; et al. Characterization of influenza virus variants induced by treatment with the endonuclease inhibitor baloxavir marboxil. *Sci. Rep.* **2018**, *8*, 9633. [[CrossRef](#)]
23. Goldhill, D.H.; te Velthuis, A.J.W.; Fletcher, R.A.; Langat, P.; Zambon, M.; Lackenby, A.; Barclay, W.S. The mechanism of resistance to favipiravir in influenza. *Proc. Natl. Acad. Sci. USA* **2018**, *115*, 11613–11618. [[CrossRef](#)] [[PubMed](#)]
24. Ma, X.; Xie, L.; Wartchow, C.; Warne, R.; Xu, Y.; Rivkin, A.; Tully, D.; Shia, S.; Uehara, K.; Baldwin, D.M.; et al. Structural basis for therapeutic inhibition of influenza A polymerase PB2 subunit. *Sci. Rep.* **2017**, *7*, 9385. [[CrossRef](#)] [[PubMed](#)]
25. Pflug, A.; Gaudon, S.; Resa-Infante, P.; Lethier, M.; Reich, S.; Schulze, W.M.; Cusack, S. Capped RNA primer binding to influenza polymerase and implications for the mechanism of cap-binding inhibitors. *Nucleic Acids Res.* **2018**, *46*, 956–971. [[CrossRef](#)]
26. Soh, Y.S.; Moncla, L.H.; Eguia, R.; Bedford, T.; Bloom, J.D. Comprehensive mapping of adaptation of the avian influenza polymerase protein PB2 to humans. *eLife* **2019**, *8*, e45079. [[CrossRef](#)]
27. Jagger, B.W.; Memoli, M.J.; Sheng, Z.-M.; Qi, L.; Hrabal, R.J.; Allen, G.L.; Dugan, V.G.; Wang, R.; Digard, P.; Kash, J.C.; et al. The PB2-E627K Mutation Attenuates Viruses Containing the 2009 H1N1 Influenza Pandemic Polymerase. *mBio* **2010**, *1*, e00067-10. [[CrossRef](#)]
28. Hoffmann, E.; Neumann, G.; Kawaoka, Y.; Hobom, G.; Webster, R.G. A DNA transfection system for generation of influenza A virus from eight plasmids. *Proc. Natl. Acad. Sci. USA* **2000**, *97*, 6108–6113. [[CrossRef](#)] [[PubMed](#)]
29. Doud, M.B.; Bloom, J.D. Accurate measurement of the effects of all amino-acid mutations on influenza hemagglutinin. *Viruses* **2016**, *8*, 155. [[CrossRef](#)]
30. Doud, M.B.; Hensley, S.E.; Bloom, J.D. Complete mapping of viral escape from neutralizing antibodies. *PLoS Pathog.* **2017**, *13*, e1006271. [[CrossRef](#)] [[PubMed](#)]
31. Hengrung, N.; El Omari, K.; Serna Martin, I.; Vreede, F.T.; Cusack, S.; Rambo, R.P.; Vonnrhein, C.; Bricogne, G.; Stuart, D.I.; Grimes, J.M.; et al. Crystal structure of the RNA-dependent RNA polymerase from influenza C virus. *Nature* **2015**, *527*, 114–117. [[CrossRef](#)]